

2013 20th Iranian Conference on Biomedical Engineering

(ICBME 2013)

**Tehran, Iran
18-20 December 2013**






**IEEE Catalog Number: CFP1318K-POD
ISBN: 978-1-4799-3233-7**



3 A B C D E F H I M N O P Q R T V 

3



3 A B C D E F H I M N O P Q R T V 

3-D electrical model of a neuroprosthesis stimulator based on the concept of stimulus router system  

3D Automatic Segmentation of Coronary Artery Based on Hierarchical Region Growing Algorithm (3D HRG) in CTA Data- sets  



A



3 A B C D E F H I M N O P Q R T V 

A 168 μ W MICS Band Transmitter Based on Injection Locking for Biomedical Sensor Nodes  

A Fully Automated Segmentation of Radius Bone Based on Active Contour in Wrist MRI Data Set  



A morphological approach for mental fatigue assessment  



A PCA-Assisted EMG-Driven Model to Predict Upper Extremities' Joint Torque in Dynamic Movements  



A Simulation study on the spatial pattern of fiber activation in response to interferential currents stimulation  



Absence epilepsy seizure onsets detection based on ECG signal analysis  

Adaptive 3D MV Beamforming in Medical Ultrasound Imaging  

Altered Connectivity of Task Related Functional Networks in Healthy Aging  

Analyzing Synergistic and Antagonistic Muscle Behavior during Elbow Planar Flexion-Extension: Entropy-assisted vs. Shift-Parameter Criterion  

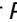

Application of Second and Higher Order Subspace Tracking in Multichannel Data Analysis  



Autonomous Detection of Heartbeats and Categorizing them by using Support Vector Machines  



B



3 A B C D E F H I M N O P Q R T V 

Bidirectional Neural Network for Pathological Voice Detection  



Blood flow simulation in a stenotic vessel surrounded by biological tissue  

Bond graph application in sports engineering: Evaluating the effects of impact parameters on tennis elbow injury  


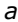
C





3 A B C D E F H I M N O P Q R T V 

CFD study of mesenchymal stem cells in fluid flow  

Characteristics of the Howland current source for Bioelectric Impedance Measurements Systems  

Characterization and evaluation of acacia gum loaded PVA hybrid wound dressing  


Comparing the Robustness of Brain Connectivity Measures to Volume Conduction Artifact  



Continuum model of actin-myosin flow  



Controlling a Drug Delivery Micropump Using Surface Acoustic Wave Correlator  

D



3 A B C D E F H I M N O P Q R T V 

Detection of Abnormalities in Wireless Capsule Endoscopy Frames using Local Fuzzy Patterns  

Detection of Motion Artifacts in fNIRS via the Continuous Wavelet Transform  

Does Deficits in Place Field Formation Cause Spatial Navigation Impairment in Alzheimer's Disease?  

E[3](#) [A](#) [B](#) [C](#) [D](#) [E](#) [F](#) [H](#) [I](#) [M](#) [N](#) [O](#) [P](#) [Q](#) [R](#) [T](#) [V](#) [⤵](#)

EEG-based Emotion Recognition Using Recurrence Plot Analysis and K Nearest Neighbor Classifier [''&&](#),

Effect of considering stability requirements on antagonistic muscle activities using a musculoskeletal model of the human lumbar spine [''&* \\$](#)

Effects of Vertebroplasty parameters on the response of multi directional loading in lumbar spine: finite element model [''&* -](#)

Estimating the heat source and the heat transfer coefficient simultaneously in a living tissue by conjugate gradient method [''%\\$-](#)

Extracting and study of synchronous muscle synergies during fast arm reaching movements [''%\)](#)

F[3](#) [A](#) [B](#) [C](#) [D](#) [E](#) [F](#) [H](#) [I](#) [M](#) [N](#) [O](#) [P](#) [Q](#) [R](#) [T](#) [V](#) [⤵](#)

Feasibility of Ti-based Metallic Glass Coating in Biomedical Applications [''&\) \\$](#)

Feature Descriptor Optimization in Medical Image Retrieval Based on Genetic Algorithm [''&, \\$](#)

H[3](#) [A](#) [B](#) [C](#) [D](#) [E](#) [F](#) [H](#) [I](#) [M](#) [N](#) [O](#) [P](#) [Q](#) [R](#) [T](#) [V](#) [⤵](#)

Heart Sound Segmentation Based on Recurrence Time Statistics [''&%\)](#)

I[3](#) [A](#) [B](#) [C](#) [D](#) [E](#) [F](#) [H](#) [I](#) [M](#) [N](#) [O](#) [P](#) [Q](#) [R](#) [T](#) [V](#) [⤵](#)

Impairment of Long-Term Potentiation in Alzheimer's Disease: a Computational Study Based on Tripartite Synapse Structure ['''' +](#)

Individual Teeth Segmentation in CBCT and MSCT Dental Images Using Watershed [''&+](#)

Investigating the Role of Foot Placement on the Muscular Forces of Knee Extensors in Horizontal Leg Press: A Static Optimization Approach ['''\) -](#)

M[3](#) [A](#) [B](#) [C](#) [D](#) [E](#) [F](#) [H](#) [I](#) [M](#) [N](#) [O](#) [P](#) [Q](#) [R](#) [T](#) [V](#) [⤵](#)

Manifold Learning for ECG Arrhythmia Recognition [''%&*](#)

Mathematical modeling of heart rate and blood pressure variations due to changes in breathing pattern ['''\) \(](#)

Measurement of mechanical properties of human saphenous vein using an inflation experiment [''%\)\)](#)

Mechanical Design, Simulation and Nonlinear Control of a New Exoskeleton Robot for Use in Upper-Limb Rehabilitation after Stroke ['''\)](#)

Modeling Blood Flow & Pressure in Systemic Circulation with Cuff Occlusion [''\(,](#)

N[3](#) [A](#) [B](#) [C](#) [D](#) [E](#) [F](#) [H](#) [I](#) [M](#) [N](#) [O](#) [P](#) [Q](#) [R](#) [T](#) [V](#) [⤵](#)

Neurophysiological Analysis of Schizophrenia Based On Dysfunction of the Glutamatergic System Using a Tripartite Synapse Model [''%' '](#)

Numerical and 1-D modeling of pulmonary circulation along with lumped parameter modeling of the heart ['''- '](#)

O[3](#) [A](#) [B](#) [C](#) [D](#) [E](#) [F](#) [H](#) [I](#) [M](#) [N](#) [O](#) [P](#) [Q](#) [R](#) [T](#) [V](#) [⤵](#)

Optimizing the Parameters of Continuous RF pulses for CEST MRI by Numerical Solution to the Bloch-McConnell Equations [''%' +](#)

P[3](#) [A](#) [B](#) [C](#) [D](#) [E](#) [F](#) [H](#) [I](#) [M](#) [N](#) [O](#) [P](#) [Q](#) [R](#) [T](#) [V](#) [⤵](#)

Personalized ECG Signal Classification Using Block-Based Neural-Network and Particle Swarm Optimization'''&\$'

Predicting Emotions Induced by Music Using System Identification Theory'''%

Predicting termination of Paroxysmal atrial fibrillation using higher order statistics in EMD domain'''&\$

Protein complex identification by graph local clustering'''&(+

Pseudo-increasing Frame Rates of Carotid Artery B-mode Images using Manifold Learning'''%(

Q



3 A B C D E F H I M N O P Q R T V ط

Quantifying variability of young and older adults during gait with Linear and Nonlinear Tools'''+%

R



3 A B C D E F H I M N O P Q R T V ط

R-R Interval Simulation Based on Power Spectrum Curve Fitting'''%&

T



3 A B C D E F H I M N O P Q R T V ط

The appropriate dimensions of the porous microchannel for blood ions separation'''%+

The representation of fuzzy model for auditory brainstem response to one syllable speech stimuli /da/''' %

Time Series Analysis of the Twinkling Artifact in Color Doppler Sonography for Surface Roughness Differentiation: An In Vitro Feasibility Study'''+*

V



3 A B C D E F H I M N O P Q R T V ط

Validation of the Saadat NIBP module according to the ANSI/AAMI-SP10 protocol'''%-

3



ط A B C D E F H I M N O P Q R T V ط

طراحی واکر کمک حرکتی جهت استفاده سالمندان و آسیب دیدگان نخاعی